Contrib Mineral Petrol (1994) 116:448–461

Contributions to Mineralogy and Petrology

Retrograde formation of NaCl-scapolite in high pressure metaevaporites from the Cordilleras Béticas (Spain)

Maria Teresa Gómez-Pugnaire[1], Gerhard Franz[2], Vicente López Sánchez-Vizcaino[1]

[1] Departamento de Mineralogía y Petrología, Facultad de Ciencias, Universidad de Granada, E-18002 Granada, Spain
[2] Fachgebiet Petrologie, Technische Universität Berlin, D-10623 Berlin, Germany

Received 10 May 1993 / Accepted 12 January 1994

Abstract. A Permo-Triassic pelite-carbonate rock series (with intercalated metabasitic rocks) in the Cordilleras Béticas, Spain, was metamorphosed during the Alpine metamorphism at high pressures (P_{min} near 18 kbar). The rocks show well preserved sedimentary features of evaporites such as pseudomorphs of talc, of kyanite-phengite-talc-biotite, and of quartz after sulfate minerals, and relicts of baryte, anhydrite, NaCl, and KCl, indicating a salt-clay mixture of illite, chlorite, talc, and halite as the original rock. The evaporitic metapelites have a whole rock composition characterized by high Mg/(Mg + Ca) ratios > 0.7, variable alkaline and Sr, Ba, contents, but are mostly K_2O rich (< 8.8 wt%). The F (< 2600 ppm), Cl (< 3600 ppm), and P_2O_5 (< 0.24 wt%) contents are also high. The pelitic member of this series is a fine grained biotite rock. Kyanite-phengite-talc-biotite aggregates in pseudomorphs developed in the high pressure stage. Albite-rich plagioclase was formed when the rocks crossed the albite stability curve in the early stages of the uplift. Scapolite, rich in NaCl (Ca/(Ca + Na) mol% 24–40) and poor in SO_4, with Cl/(Cl + CO_3) ratios between 0.6 and 0.8, formed as porphyroblasts, sometimes replacing up to 60% of the rock in a late stage of metamorphism (between 10 and 5 kbar, near 600°C). No reaction with albite is observed, and the scapolite formed from biotite by:

Al-biotite + $CaCO_3$ + NaCl + SiO_2
= Al-poor biotite + scapolite + $MgCO_3$ + KCl + $MgCl_2$ + H_2O

Calculated fluid composition in equilibrium with scapolite indicates varying salt concentrations in the fluid. Distribution of Cl and F in biotite and apatite also indicates varying fluid compositions.

Introduction

Minerals of the scapolite group have received considerable attention in the last years in petrological studies because of their potential as a temperature indicator for granulite facies conditions (CO_3-scapolite) and their ability to act as a source or sink for a fluid phase (CO_3, SO_4, Cl) in a wide variety of metamorphic environments: e.g., Moecher and Essene (1991) for granulite terranes and xenoliths; Oterdoom and Wenk (1983) for regionally metamorphosed carbonate rocks; Vanko and Bishop (1982) for hydrothermal-igneous scapolitization; Mora and Valley (1989) for metaevaporites. Metaevaporites are potentially suitable for NaCl-scapolite (marialite) formation and thus useful for studying the relationships between scapolite-plagioclase-halite reactions, metamorphic conditions, and the nature of the fluid phase.

In the Cordilleras Béticas in southern Spain, the western part of the Alpine-Himalayan chain, we found scapolite-bearing rocks in metaevaporites, which can be traced regionally over several kilometers. They form a stratigraphic horizon, though with considerable variation in thickness (Nijhuis 1964; Gómez-Pugnaire et al. 1981b; Gómez-Pugnaire and Cámara 1990) at the base of a thick Triassic marble unit. The whole unit was subjected to high pressures, whereas scapolite grew during a late stage. This allows us to make some constraints on marialite stability. The crystal chemistry of the minerals from this locality is described in order to decipher the metamorphic history with special emphasis on scapolite and the fluid phase.

Geological setting

The sample locality is situated near the village of Cóbdar in the Nevado-Filábride complex, the lowermost tectonic unit of the Cordilleras Béticas (Fig. 1; Balanya and Garcia-Dueñas 1986). The Alpujárride and the Maláguide complexes form the higher tectonic units. The Nevado-Filábride complex consists of a pre-Permian basement and a Permo-Triassic upper sequence. The contact between them is an erosion surface, now discordant and almost completely obliterated during metamorphism (Egeler 1963; Gómez-

Correspondence to: G. Franz

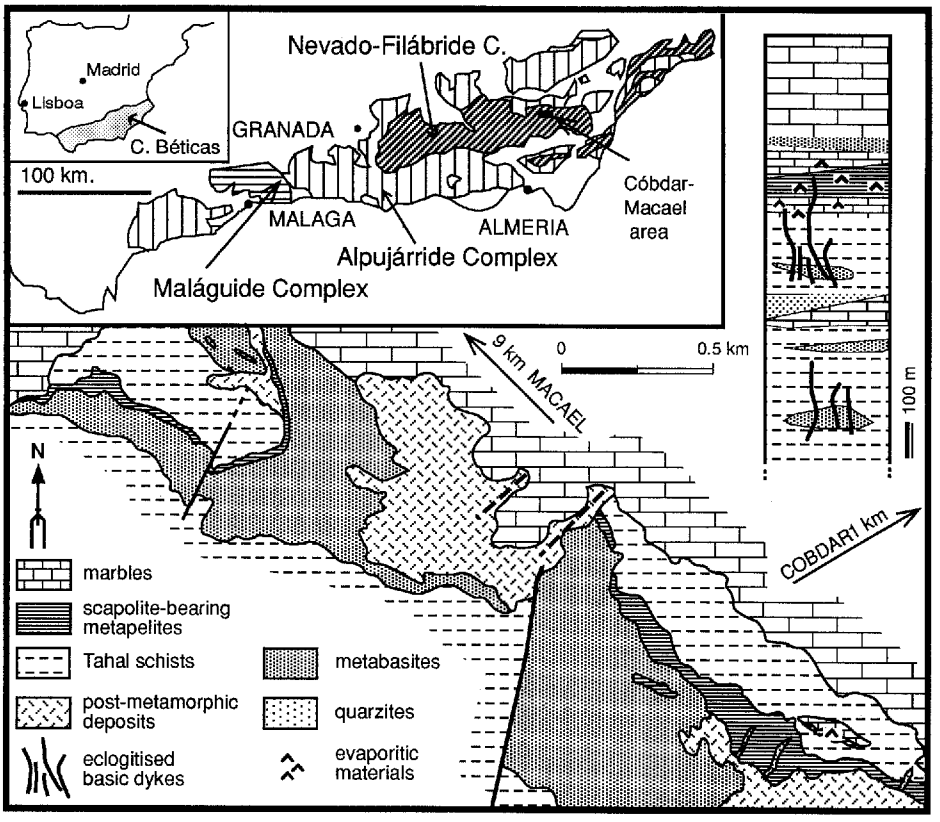

Fig. 1. Geological sketch map of the sample locality of the scapolite occurrence near Cóbdar and a generalized stratigraphic profile (quartzites, which are indicated in the profile, are too small to be represented in the map). The *inset* shows the major tectonic units of the Cordilleras Béticas

Pugnaire et al. 1981a). The base of the Permo-Triassic consists of quartz-feldspar-rich schists, quartzites, and intercalated metaconglomerates ("Esquistos de Tahal", Nijhuis 1964, see stratigraphic column in Fig. 1). There are also intercalated metabasites as doleritic-gabbroic sills, porphyritic dykes, and large bodies of irregular form. The upper part is a thick unit of mostly pure and coarse grained marble with minor intercalations of metapelites (not shown in Fig. 1) and metabasites. Between the lower and the upper part is a gradational transition from the Esquistos de Tahal into a more varied series of impure marbles, quartzites, and very fine grained metapelites, which is interpreted as a metaevaporite sequence.

All rocks were metamorphosed and folded during the Alpine metamorphism. All contacts are strongly deformed, and the original sedimentary sequence is tectonically disturbed. However, in the Cóbdar area, where these rocks reach a maximal thickness, we think that they represent in general a more or less coherent sequence, typical for a shallow marine environment, which was deposited onto sediments of continental affinity (Gómez-Pugnaire et al. 1978; Muñoz 1986; De Jong and Bakker 1991). There are no indications of large scale tectonic movements, and from this point of view the situation is similar to other areas of the Nevado-Filábride complex (Gómez-Pugnaire 1981; Vissers 1982; Galindo-Zaldivar 1990; Jabaloy 1990).

The Alpine metamorphism of the Nevado-Filábride complex generally evolved from a high pressure metamorphism at relatively low temperatures (Nijhuis 1964) to conditions of approximately 6 kbar/600°C (Gómez-Pugnaire 1981). The *P-T* conditions of the high pressure event were determined mainly in mafic rocks, where the eclogitic relicts are best preserved, and estimates range between 11–16 kbar/600–640°C (Vissers 1982; Gómez-Pugnaire and Fernandez-Soler 1987; Puga et al. 1989; De Jong 1991). In the study area no detailed investigations are available; preliminary data indicate about 20–22 kbar/650°C (Galindo et al. 1991).

Petrography

The metapelites of the metaevaporite sequence generally do not show a preferred mineral orientation due to the small grain size of the matrix material. Only in the vicinity of retrograde deformation zones they may show a slight foliation, and if they are rich in amphibole this mineral also has a preferred orientation. Aggregates of talc that form pseudomorphs are commonly aligned. Extension veins are filled with amphibole (sometimes with sigmoidal growth), plagioclase, carbonate, talc, biotite, epidote, quartz, and apatite.

The grey to greenish-brownish evaporitic metapelites are porphyroblastic with a fine grained matrix of biotite (0.2–0.5 mm), subordinate amounts of white mica, talc, tremolitic amphibole, quartz, calcite, titanite, rutile, tourmaline, apatite, hematite, iron sulfide, and round or almond-shaped blasts of scapolite up to 1 to 2 cm in diameter (Fig. 2). The distribution of scapolite in the rocks is irregular. Sometimes the blasts completely disappear within a distance of a few meters, sometimes they are in horizons, where they can form up to 60% of the mode and are rather small crystals (< 0.5 mm). These horizons alternate with layers devoid of scapolite. Towards the contact with carbonate rocks (which occur in layers of < 0.5 m), the size of the scapolite crystals and associated tremolite increases to 5 to 6 cm. The scapolite blasts may also enclose the above mentioned extensional veins.

Other minerals, which may form porphyroblasts, are plagioclase (An < 27 mol%), chlorite, and tourmaline, but they occur less frequently. Tourmaline blasts are sometimes surrounded by a rim of scapolite. Plagioclase blasts are generally smaller than scapolite and can be included in scapolite (Fig. 3). The major scapolite-bearing rock types are:

1. Metapelites (biotite matrix) with
- scapolite as the only porphyroblast
- plagioclase ± scapolite ± chlorite
- tourmaline ± scapolite
- Na-Ca amphibole + plagioclase ± scapolite
- tremolite + carbonate ± scapolite

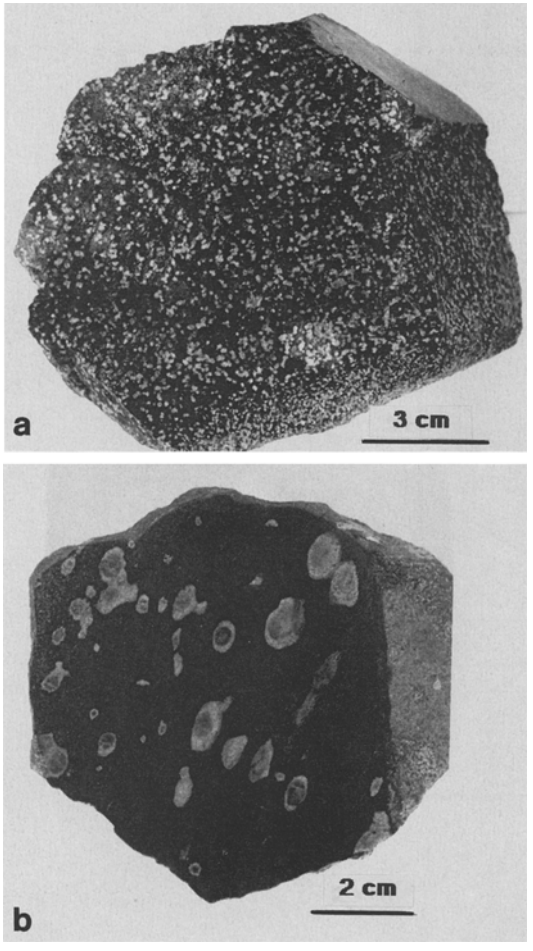

Fig. 2a, b. Hand specimens of scapolite-rich metaevaporites with mm- and cm-size scapolite porphyroblasts in a biotite matrix

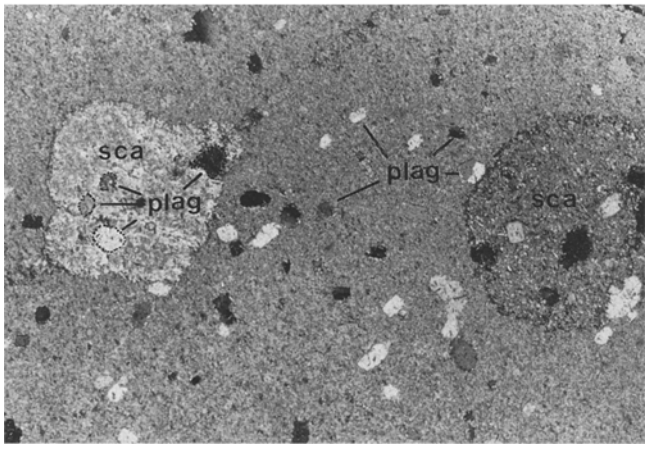

Fig. 3. Photomicrograph: scapolite blasts, *sca*, in a matrix composed dominantly of biotite with small albite-rich plagioclase, *plag*, (outlined in the left scapolite crystal) blasts. Scapolite replaces the biotite matrix, but not plagioclase, which is of identical composition, shape, and grain size in both the matrix and as inclusions in the scapolite (sample no. 87 Cob 20; length of photo 2.6 mm, crossed nicols)

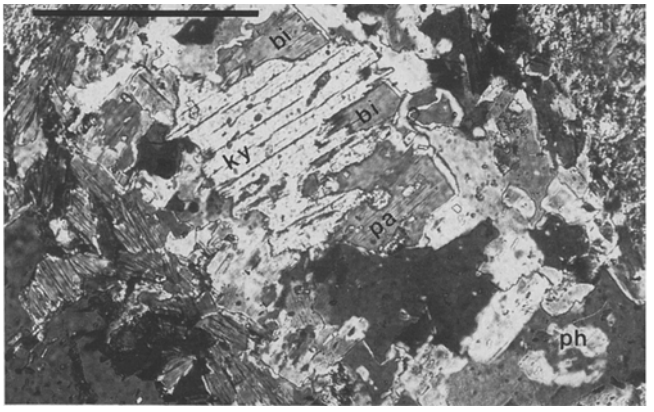

Fig. 4. Photomicrograph: kyanite, *ky*, and phengite, *ph*, which occur in tabular pseudomorphs after sulfate minerals, are replaced by biotite, *bi*, and paragonite, *pa*. Inclusions in kyanite and talc are baryte and anhydrite (sample no. Cob 55/1a; *scale bar* 0.2 mm, crossed nicols)

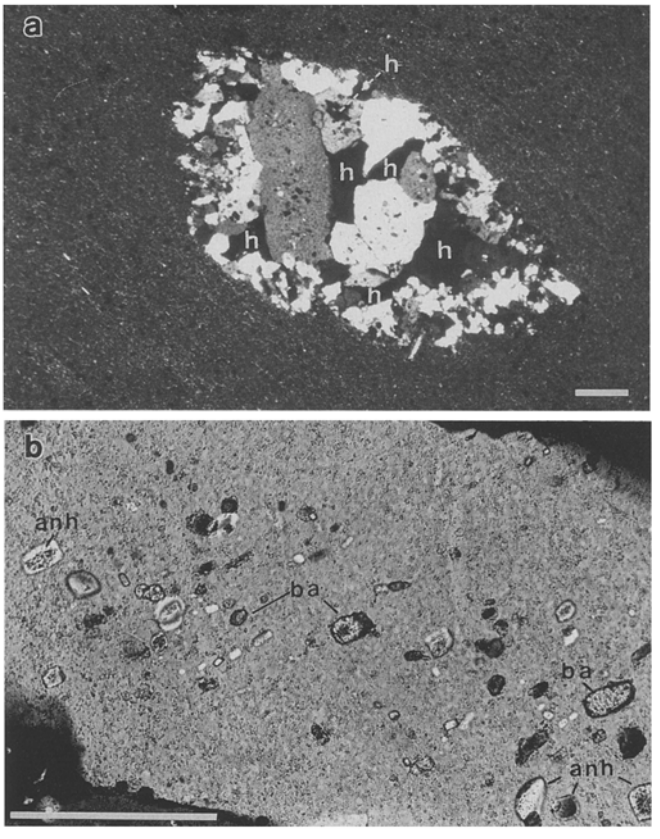

Fig. 5. a Photomicrograph: quartz aggregate in a biotite matrix, showing the small grain size at the rim of the aggregate and large crystals in the center. Holes, *h*, contain remnants of chloride (NaCl and KCl, see Fig. 7). **b** Enlarged part of a quartz crystal, showing baryte, *ba*, and anhydrite, *anh*, inclusions (sample no. Ul 14 a, b; *scale bar* 0.2 mm, crossed nicols)

- scapolite + kyanite + talc + phengite + biotite (+ secondary chlorite)
- scapolite + garnet

2. Marbles and calc micaschist

- scapolite + plagioclase
- scapolite + tremolite ± epidote

We could not find any systematic relationship between the different rock types, especially in respect to the scapolite-plagioclase-

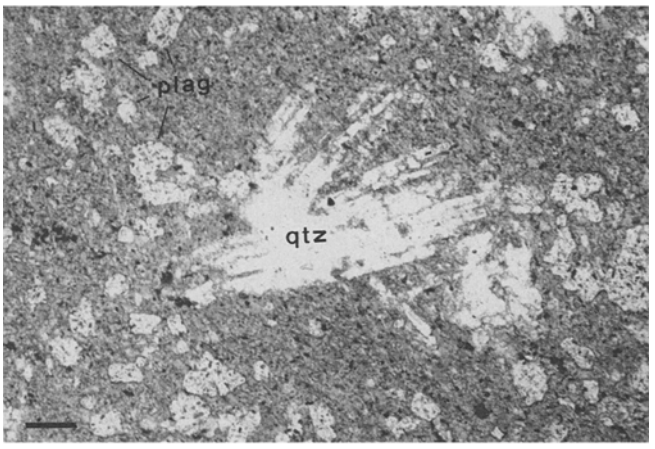

Fig. 6. Photomicrograph of a tabular, polycrystalline quartz pseudomorph, *qtz*, with a "bird tail shape", in a biotite matrix together with plagioclase, *plag*, blasts. (sample no. Cob 50/5c; *scale bar* 0.2 mm, plain polarized light)

carbonate abundance and distribution. The changes can occur along and across strike over a few cm distance, and seem to be unrelated to tectonic features such as deformation zones or to lithological contacts of the metabasites.

An especially interesting rock type of the metaevaporites is rare and probably represents less than 5% of the whole exposed sequence. It contains platy pseudomorphs of kyanite-talc-biotite-phengite-paragonite and secondary chlorite + quartz (Fig. 4) as well as tabular aggregates of talc with inclusions of baryte and anhydrite. Aggregates of quartz, irregular (Fig. 5) and platy (Fig. 6) in shape, with minor amounts of carbonate and inclusions of baryte, anhydrite, apatite, talc, and phlogopite, as well as aggregates of plagioclase + apatite ± epidote appear frequently in all the lithologies. The size of the tabular quartz pseudomorphs ranges from mm to several cm and the former crystals were euhedral with a platy or tabular form, often oriented radially around carbonate. The shape as well as the mineralogy of the pseudomorphs suggests that they were formed after sulfate minerals such as baryte and gypsum or anhydrite. Replacement of the sulfate phases by quartz or other minerals could have occurred either at an early stage during diagenesis, or during the metamorphic evolution. In any case, the well preserved shape is a strong indication of sulfate minerals, which are typical for an evaporitic environment.

In the irregular quartz aggregates (Fig. 5) grain size increases from the rim toward the center, and they often show holes. Special care was taken to distinguish between holes produced by the thin section preparation and original vacuoles. Scanning electron microscopy on polished thin sections, prepared with the method described by Trommsdorf et al. (1985), revealed that the holes were originally present in the rock. Figure 7a shows intergrown quartz crystals from Fig. 5a with relicts of KCl. In Fig. 7b relicts of NaCl are shown with a characteristic cross shape. Due to the fine grain size of the rocks, no fluid inclusions suitable for heating and freezing experiments were found.

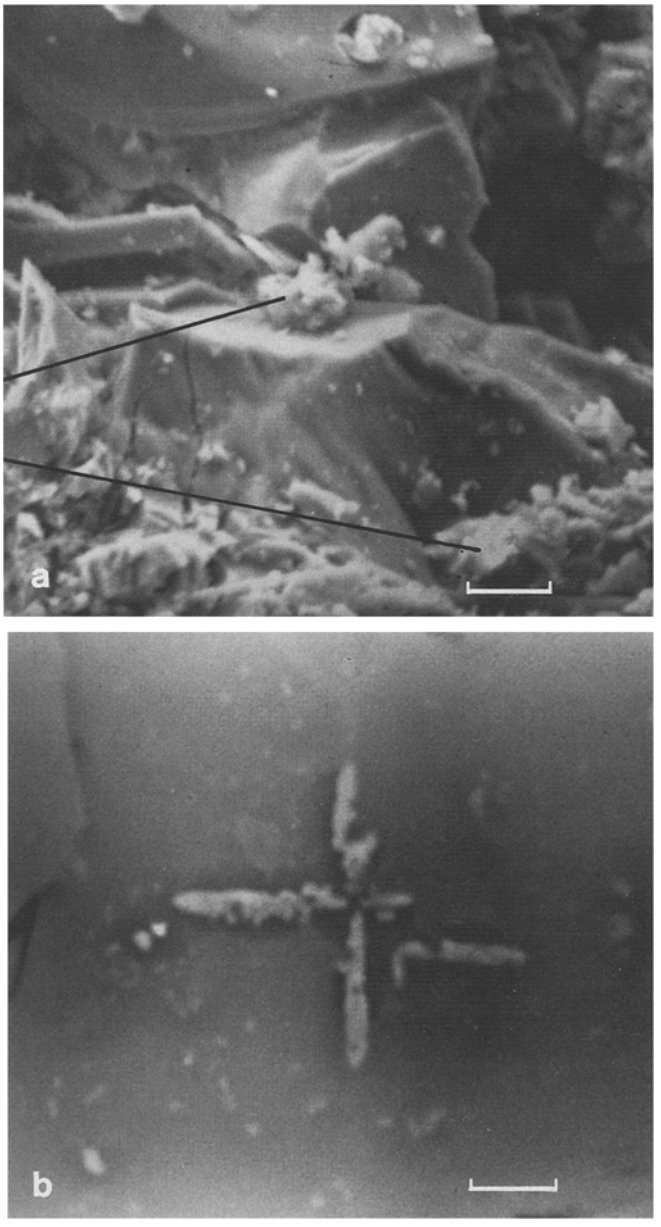

Fig. 7a, b. Scanning electron microscopy photographs of quartz crystals forming irregular or oval shaped aggregates (see Fig. 5). In depressions on the surface of the quartz crystals KCl (**a**) and NaCl (**b**) could be identified by energy dispersive analysis. *Lines* in (a) point to the analyzed crystals. *Scale bar* is 5 μm; sample no.CH 2)

Whole rock composition

Twenty-five specimens were selected for determination of major and some trace elements (F, Cl, S, Sr, Ba) by X-ray fluorescence spectroscopy using a fully automated Phillips PW1404 spectometer and fused disks with lithium tetraborate as a flux medium. The elements F, Cl, S, Sr and Ba were determined on pressed powder pellets using an elvacite solution in acetone as binder. Precision for major elements is estimated to be better than 2% relative except for Al, Na, Mn, and P_2O_5 (5% relative). For Cl and F determinations, precision is about 1% relative at the 1000 ppm level. The results are presented in Table 1. Figure 8 shows the Ca-Mg-Al ratios of the rocks (Moine et al. 1981). The Mg/(Mg + Ca) ratio is high, especially in rocks with kyanite (> 0.92) or in rocks with white mica in the matrix. The sum of MgO + Fe_2O_3 varies between 10 and 20 wt%, and the A-F-M diagram (inset in Fig. 8; projection from muscovite, quartz, H_2O; F = FeO_{total}) clearly shows their Mg-rich composition. Also the amount of alkalis and the Na_2O/K_2O ratios are highly variable, but in most cases the amount of potassi-

Table 1. Whole rock composition, determined by XRF. Analyses 1, 2, 4, 9, 10, 22, 23 and 24 taken from Gómez-Pugnaire and Cámara (1990, Table 1)

Sample	Plagioclase-bearing metapelites								Kyanite + talc + phengite metapelites			
	61/2 1	50/4 2	50/6a 3	50/6D 4	CH-28 5	CH-29A 6	C-13 7	UL-2 8	55/1 9	14/2a 10	14/2a 11	CB-55a 12
SiO_2	53.50	57.00	52.64	52.30	51.98	50.44	50.72	53.75	48.30	50.00	50.57	43.36
TiO_2	0.94	1.00	0.95	1.01	0.98	1.02	0.99	0.99	0.93	0.78	0.72	1.13
Al_2O_3	18.30	18.4	19.94	19.90	18.11	20.65	19.14	18.85	19.70	16.10	13.15	20.00
Fe_2O_3	7.20	5.11	4.56	4.35	9.33	6.08	5.49	4.92	4.84	6.23	5.68	8.13
MgO	6.43	5.42	8.03	6.71	5.34	6.42	8.04	6.57	13.50	16.50	20.63	14.28
MnO	0.02	0.02	0.09	0.01	0.04	0.02	0.02	0.05	0.02	0.02	0.08	0.10
CaO	2.34	2.28	3.21	2.65	2.66	2.12	3.07	2.62	1.56	0.73	0.56	0.80
Na_2O	3.67	1.70	2.10	4.24	1.66	5.50	2.38	1.26	2.67	1.17	0.64	0.28
K_2O	4.88	6.01	5.91	5.11	6.32	4.36	6.28	6.39	3.65	4.33	3.92	8.8
P_2O_5	0.22	0.18	0.24	0.21	0.20	0.22	0.24	0.22	0.24	0.22	0.15	0.19
L.O.I.	2.36	2.73	2.47	3.12	2.58	1.86	2.46	2.83	4.57	3.76	3.90	2.93
Total	99.86	99.85	100.14	99.61	99.2	98.69	98.83	98.45	99.98	99.84	100.00	100.00
Ppm												
F	ND	ND	1700	ND	1200	1200	2300	1600	ND	ND	500	2000
Cl	ND	ND	3660	ND	2760	2050	2400	1730	ND	ND	1130	1580
S	ND	ND	260	N.D.	0	80	105	50	ND	ND	180	0
Sr	ND	ND	380	ND	195	441	409	283	ND	ND	427	245
Ba	833	ND	259	ND	624	258	330	734	ND	ND	1309	918

Table 1 (continued)

Sample	Metapelites with plagioclase + white mice in the matrix					Marbles				Carbonate ± apatite ± amphibol metapelites			
	UL-16 13	CH-35 14	52/1b 15	UL-10 16	CH-5 17	CB-GW 18	CB-HB 19	GW 20	UL-12 21	61/1 22	55/4 23	CB-27 24	CH-7 25
SiO_2	55.94	55.16	52.48	52.40	57.36	12.50	8.78	10.51	53.98	55.3	55.40	49.50	51.13
TiO_2	0.84	0.91	0.95	1.02	1.04	0.19	0.14	0.22	0.88	0.83	0.76	0.91	0.93
Al_2O_3	16.70	20.27	20.01	21.84	17.13	4.54	3.69	4.53	15.68	16.00	15.70	17.90	17.56
Fe_2O_3	6.01	7.34	9.69	7.89	4.85	1.50	2.15	2.06	7.21	7.50	6.40	8.16	6.38
MgO	7.71	5.93	6.40	4.99	7.02	2.96	0.05	3.46	8.62	8.13	8.71	9.74	9.28
MnO	0.03	0.09	0.12	0.08	0.02	0.02	3.66	0.00	0.04	0.04	0.06	0.04	0.08
CaO	1.12	0.44	0.53	0.46	1.30	40.00	41.50	44.73	3.22	3.32	3.25	3.56	3.68
Na_2O	1.14	0.45	0.36	0.19	3.00	0.35	0.74	0.49	1.09	1.78	1.00	1.05	1.74
K_2O	6.74	6.38	6.46	7.68	5.08	0.83	0.12	1.19	5.42	4.95	4.80	5.91	6.05
P_2O_5	0.19	0.17	0.14	0.13	0.17	0.06	0.05	0.11	0.19	0.23	0.20	0.23	0.23
L.O.I.	2.75	2.86	2.86	3.31	2.43	36.70	38.80	31.71	2.75	1.91	2.61	2.98	2.66
Total	99.17	100.00	100.00	99.99	99.40	99.65	99.68	99.01	99.08	99.99	98.89	99.98	99.72
Ppm													
F	1200	ND	800	1100	ND	ND	ND	2600	1000	ND	ND	ND	1100
Cl	1140	ND	1070	520	ND	ND	ND	580	1830	ND	ND	ND	1230
S	245	152	0	0	115	ND	ND	1360	40	ND	ND	ND	0
Sr	169	531	164	84	305	ND	ND	2242	158	ND	ND	ND	179
Ba	732	199	540	320	207	ND	ND	129	579	ND	ND	ND	528

L.O.I., loss on ignition; ND, not determined

um is much higher than that of sodium. The magnesian rock composition explains the absence of minerals such as staurolite and chloritoid, the scarcity of garnet, and the abundance of phlogopite and talc. Sedimentary or diagenetic precursor minerals for the observed metamorphic assemblages were probably illite + talc + chlorite (see discussion). The sediments must have been carbonate poor, as indicated by the dashed arrow in Fig. 8, which separates carbonate-bearing sediments from carbonate-free evaporites. The field of sulfate-bearing evaporites (outlined by dashed lines in Fig. 8, Moine et al. 1981) is not of great relevance for our study, because it relates to carbonate-bearing rocks only. If it is extrapolated into the field of carbonate-free evaporites, the analysis points

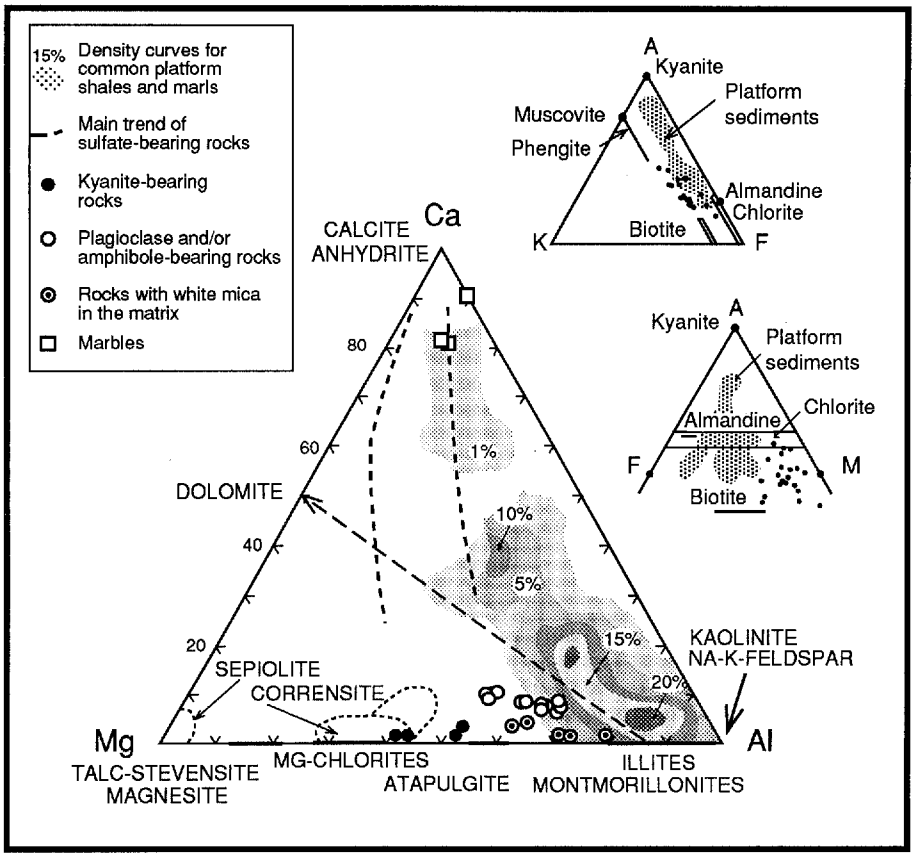

Fig. 8. Whole rock composition in terms of Ca, Mg, and Al (in milliatoms, Moine et al. 1981), and in an A (= Al_2O_3), K (= K_2O), F (= FeO + MgO) projection, and an A (= Al_2O_3), F (= FeO), M (= MgO) diagram (+ quartz, muscovite, H_2O). The diagrams also show the fields of typical argillites and platform sediments, as well as the compositions of the most important precursor minerals. The *arrow (dashed)* separates the field of carbonate-bearing from carbonate-poor or carbonate-free rocks (Moine et al. 1981)

for the rocks with pseudomorphs would fall into this field. Phosphate is rather constant near 0.2 wt% and reflects the large amount of accessory apatite. Serdyuchenko (1975) also found 0.25 wt% P_2O_5 in metaevaporites.

The F-contents vary between 1000 and 2300 ppm, and are significantly higher than in average platform sediments (800 ppm; Moine et al. 1981). The Cl-contents vary between 520 and 3660 ppm. Similarly high values are typical for metaevaporites (Serdyuchenko 1975:0.28 and 0.49 wt%; Hogarth and Griffin 1978:0.07 to 0.86 wt%). The Cl is present in the rock in scapolite, biotite, and in apatite as well as in solid NaCl and KCl inclusions (Fig. 7). The highest contents of S and Sr were found in a marble (1360 and 2242 ppm, respectively), indicating the presence of sulfate minerals. In general, the amounts of these elements, as well as those of Ba, are very variable and reflect the presence or absence of baryte and anhydrite inclusions. Calcium sulfate is abundant in marbles from the whole Cóbdar-Macael area (Voet 1976).

Boron and lithium are also key elements for the sedimentary environment (Moine et al. 1981), but due to the lack of analytical facilities they have yet to be analyzed. The large modal amount of tourmaline, however, clearly indicates that the B contents are high.

Mineral chemistry

Minerals were analyzed with an automated Camebax electron microprobe (wave length dispersive system) with natural minerals and synthetic materials as standards (Na = albite; K = orthoclase; Ca and Si = wollastonite; Al = Al_2O_3; Mg = MgO; Fe = FeO; Mn = Mn; Ti = TiO_2; Cl = NaCl; S = FeS_2; F = CaF_2 and Durango fluorapatite, Sr = celestine) at 15 kV, 20 nA, using the PAP correction, at ZELMI (Techn. Univ. of Berlin). Counting times were 10 s for Na, Mg, Si, Al, Cl, K, and S; 20 s for Fe, Mn, and Ca; and 30 s for F and Ti. Additional data were obtained at the electron microprobe laboratories of Granada (chlorites and scapolite) and Edinburgh (apatite) under similar conditions. Mineral analyses of scapolite are presented in Table 2. All other tables with mineral analyses are available on request from G.P.

Scapolite

Scapolite contains inclusions of all matrix minerals, of carbonate, and also of smaller euhedral plagioclase blasts. Chlorite and the chlorite + quartz aggregates are generally not included, indicating that scapolite formed after the matrix minerals and after plagioclase, but before or probably simultaneously with chlorite. No reaction relationships with plagioclase were observed. Scapolite composition, expressed as X_{An} mol% [Ca/(Ca + Na) *100], varies mostly between 28 and 40 mol% (Table 2). There are no large differences between rocks with or without plagioclase and/or calcite (Fig. 9). Scapolite crystals in contact only with albite-rich plagioclase can be relatively rich in Na-component (mol% An below 28; minerals analyzed at the contact near the grain boundary), but there are also many crystals with relatively high Ca-contents.

Sulfer contents (in terms of atoms per formula unit) do not exceed 0.05, and are very often below the detection

Table 2. Representative electron microprobe analyses of scapolite (formulae calculated on the basis of Si + Al = 12). CB-14/2a, CB-55A, kyanite + talc + phengite + scapolite-bearing metapelites; CB-61, CB-62, other scapolite-bearing metapelites; CB-27, carbonate + plagioclase + scapolite-bearing metapelites; CB-HB, CW, UL-23, scapolite-bearing marbles

Sample	CB-14/2a			CB-61	CB-52	CB-27	CB-HB		CG-GW		UL-23		CG-55A		
SiO_2	55.15	55.53	55.69	60.39	55.08	54.63	54.62	54.95	56.31	56.98	54.52	54.97	55.25	55.13	54.93
TiO_2	0.03	0.04	0.04	0.00	0.03	0.00	0.04	0.00	0.05	0.00	0.00	0.01	0.04	0.01	0.07
Al_2O_3	23.43	23.23	23.36	20.64	22.78	23.14	23.44	23.41	22.54	22.03	23.62	23.55	23.37	22.55	22.83
FeO	0.06	0.01	0.05	0.02	0.19	0.06	0.02	0.05	0.02	0.00	0.01	0.02	0.07	0.04	0.68
MgO	0.02	0.00	0.00	0.00	0.00	0.00	0.01	0.06	0.00	0.03	0.00	0.00	0.00	0.00	0.00
MnO	0.00	0.00	0.00	0.02	0.02	0.00	0.00	0.00	0.00	0.00	0.01	0.00	0.06	0.02	0.02
CaO	8.17	7.43	8.09	7.39	7.47	8.10	8.48	8.54	5.81	5.91	9.02	8.44	7.17	8.15	8.90
Na_2O	9.20	9.87	9.29	8.19	9.84	9.10	8.85	8.82	9.98	10.06	8.72	8.96	7.88	7.65	7.88
K_2O	0.29	0.30	0.30	0.70	0.31	0.37	0.42	0.46	0.57	0.49	0.41	0.32	0.21	0.20	0.18
F	0.03	0.00	0.04	0.00	0.00	0.00	0.01	0.03	0.02	0.00	0.06	0.04	0.00	0.00	0.02
Cl	2.93	3.17	3.14	2.66	2.93	3.03	3.09	2.87	3.34	3.31	2.55	2.77	3.50	3.09	2.79
SO_3	0.32	0.43	0.28	0.31	0.36	0.26	0.39	0.35	0.00	0.01	0.00	0.00	0.25	0.50	0.16
Total	99.63	100.01	100.28	100.32	99.01	98.69	99.37	99.54	98.64	98.82	98.92	99.08	97.80	97.34	98.46
O = Cl	0.66	0.72	0.71	0.60	0.66	0.68	0.70	0.65	0.75	0.75	0.58	0.62	0.79	0.70	0.63
O = F	0.01	0.00	0.02	0.00	0.00	0.00	0.00	0.01	0.01	0.00	0.03	0.02	0.00	0.00	0.01
Total	98.96	99.29	99.55	99.72	98.35	98.01	98.67	98.88	97.88	98.07	98.32	98.44	97.01	96.64	97.82
Si	7.995	8.037	8.029	8.554	8.067	8.003	7.968	7.988	8.153	8.243	7.943	7.973	8.007	8.096	8.054
Al	4.005	3.963	3.971	3.446	3.933	3.997	4.032	4.012	3.847	3.757	4.057	4.027	3.993	3.904	3.946
Ti	0.003	0.004	0.004	0.000	0.003	0.000	0.004	0.000	0.005	0.000	0.000	0.001	0.004	0.001	0.008
Fe^{2+}	0.007	0.001	0.006	0.002	0.023	0.007	0.002	0.006	0.002	0.000	0.001	0.002	0.008	0.005	0.083
Mg	0.004	0.000	0.000	0.000	0.000	0.000	0.002	0.013	0.000	0.006	0.000	0.000	0.000	0.000	0.000
Mn	0.000	0.000	0.000	0.002	0.002	0.000	0.000	0.000	0.000	0.000	0.001	0.000	0.007	0.002	0.002
Ca	1.269	1.152	1.250	1.122	1.172	1.272	1.326	1.330	0.901	0.916	1.408	1.312	1.113	1.282	1.398
Na	2.586	2.770	2.597	2.249	2.794	2.585	2.504	2.486	2.802	2.822	2.463	2.520	2.214	2.178	2.240
K	0.054	0.055	0.055	0.126	0.058	0.069	0.078	0.085	0.105	0.090	0.076	0.059	0.039	0.037	0.034
F	0.014	0.000	0.018	0.000	0.000	0.000	0.005	0.014	0.009	0.000	0.028	0.018	0.000	0.000	0.009
Cl	0.720	0.777	0.767	0.638	0.727	0.752	0.764	0.707	0.819	0.811	0.630	0.681	0.860	0.769	0.693
SO_4	0.035	0.047	0.030	0.033	0.040	0.029	0.043	0.038	0.000	0.001	0.000	0.000	0.027	0.055	0.018
Ca/(Ca + Na)	0.329	0.294	0.325	0.333	0.296	0.330	0.346	0.349	0.243	0.245	0.364	0.342	0.335	0.371	0.384

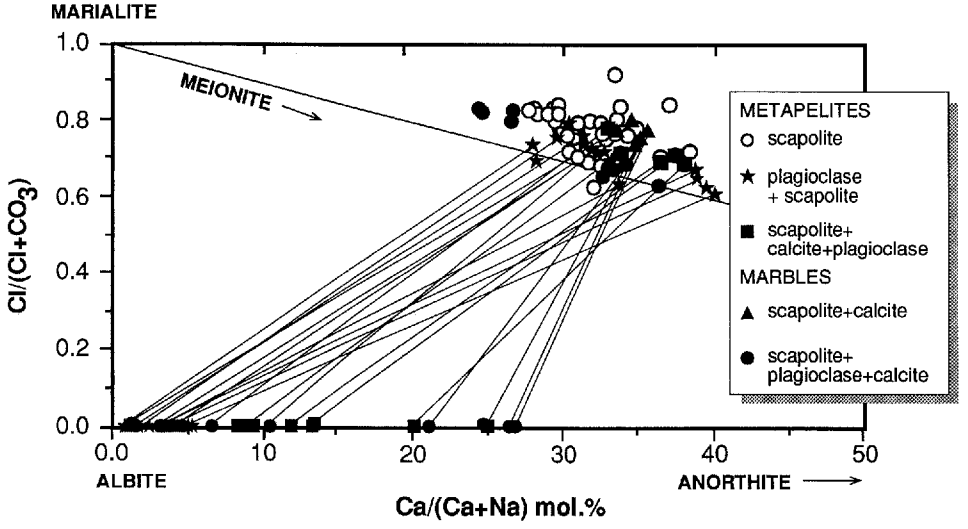

Fig. 9. Composition of scapolites, expressed as Ca/(Ca + Na) mol% and Cl- and CO_3-scapolite (SO_4-scapolite is negligible) and coexisting plagioclases. The *tie line* shows the theoretical solid solution limits between marialite and meionite according to Evans et al. (1969)

limit (estimated as < 0.05 wt%). Carbonate-scapolite, ranging between approximately 10 and 40 mol% was calculated by difference. In Fig. 9, most analyses exceed the theoretical solid solution limits proposed by Evans et al. (1969): they have more Cl-scapolite as defined by the endmembers marialite and meionite. This excess in Cl seems to be common in many natural marialitic scapolites (Evans et al. 1969; Vanko and Bishop 1982; Mora and Valley 1989; and references therein), and Ellis (1978) described synthetic scapolites in the range 30 to 85 X_{An} mol%, which also have a significant excess of Ca and Cl, as a possible endmember 3An·NaCl. This deviation in

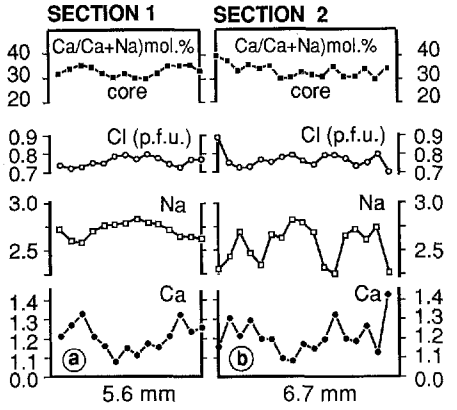

Fig. 10. Compositional zoning profile of two scapolite porphyroblasts in a biotite matrix in terms of Ca/(Ca + Na) mol% and atoms per formula unit (sample no. 87 cob 14/2)

composition of natural scapolites from the theoretical stoichiometry is explained by Chamberlain et al. (1985) as the result of local charge balance between Ca^{2+}, Na^{+} cations and Cl^{-}, CO_3^{2-} anions. The F-content is mostly near or below the detection limit (estimated as < 0.05 wt%).

Potash contents are low and correspond to an average of K/(K + Ca + Na) = 0.01. The sum of K + Ca + Na is in most cases near 3.9 (see also Mora and Valley 1989), indicating either a slight deficiency in this position or analytical problems due to evaporation of Na.

Scapolite from many samples shows optical zoning with a slight continuous decrease of birefringence toward the rim and with a higher concentration of inclusions in the central part of the crystal. Two large crystals were checked for chemical zoning (Fig. 10), which in one case is regular, with a central Na- and Cl-rich zone, an increase of Ca toward the rim, and a decrease in the outer rim. The second crystal is less regularly zoned. Another sample was found that exhibits a more complex type of zoning.

Plagioclase

Plagioclase occurs in different textural positions. Small, euhedral porphyroblasts and aggregates with apatite in the metapelites are albite with up to 10 mol% An. Plagioclase coexisting with calcite and scapolite varies between 15 and 27 mol% An. In the marbles, the plagioclases are zoned from albite-rich cores to An 35. Plagioclases are more sodic than coexisting scapolite.

Biotite

Biotite is the most abundant matrix mineral and contributes to the pseudomorphs in kyanite-bearing metapelites. It is rich in phlogopite component. The Mg/(Mg + Fe) ratio in different samples varies between 0.66 and 0.88, but the variation within a sample is small (Fig. 11). The Al^{VI}-content shows a large scatter, especially in the rocks with pseudomorphs. The Ti-content does

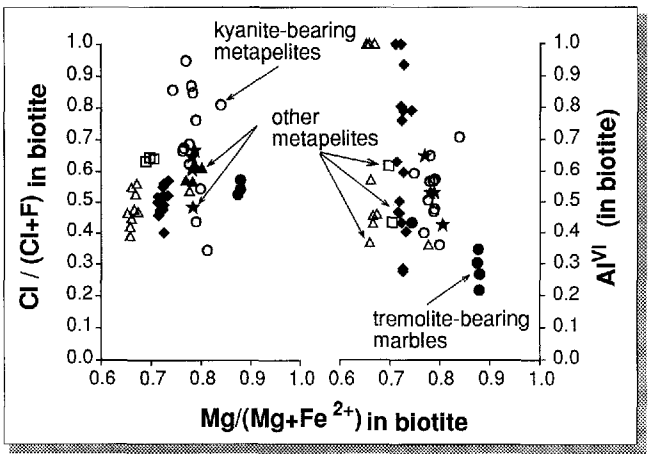

Fig. 11. Composition of biotite (cations p.f.u.); the Mg/(Mg + Fe) ratio is predominantly controlled by whole rock composition; the large variation of the Al^{VI}-content by Tschermaks exchange with the local assemblage in a sliding reaction (see text). The Cl/(Cl + F) ratios vary independently of Mg and Fe

not exceed 0.2 atoms per formula unit. All biotites contain uniformly high amounts of Cl between 0.5 and 0.8 wt%, but F ranges from below detection to 0.4 wt%. In most cases, the Cl/(Cl + F) ratio varies independently from Mg/(Mg + Fe) (Fig. 11). Only in the rocks with the kyanite pseudomorphs does a slight negative correlation exist.

White mica

White mica is rare in the matrix compared to biotite. Only in one rock with garnet does it form up to 50% of the mode in the matrix. Most of the white micas (phengite and paragonite) were found in the pseudomorphs, coexisting with talc and biotite. Paragonite is more abundant, and contains only small amounts (< 3 mol%) of margarite. The sum of Mg + Fe is also small, near 0.1 per formula unit (p.f.u., on the basis of 22 oxygens). The Si-content of the phengites varies between 6.5 and 6.8, the paragonite content between 5 and 10 mol%.

Talc

Talc was rarely identified in the matrix (probably because of the small grain size), but often occurs as inclusions in scapolite. It also contributes to the pseudomorphs, where it contains inclusions of baryte and anhydrite or is intergrown with these minerals and quartz. It always contains small amounts of Na (< 0.06 p.f.u.) and Al (< 0.3 p.f.u.). It is not clear, whether these components are present as paragonite or Na-biotite intergrowths, or are true solid solution components.

Chlorite

Chlorite is a late stage mineral in most samples. It coexists with quartz and replaces the kyanite pseudo-

morphs, or may form small porphyroblasts (with quartz inclusions). In carbonate rocks, it replaces tremolite or forms isolated crystals in the carbonate matrix. The chlorites are Mg-rich.

Garnet

Garnet is rare in the rocks. It appears in small crystals in the matrix or as inclusions in scapolite. Zoning is not distinct, and the average composition is $Alm_{64}Py_{17}Sp_4Gro_{15}$.

Amphibole

Tremolitic hornblende is relatively abundant in carbonate-bearing rocks. In the metapelites it occurs as inclusions in scapolite, in the matrix intergrown with biotite, in aggregates with plagioclase, and in veins. Zoned crystals are barroisitic in the core and more calcic in the rim (edenite to Mg-hornblende).

Accessory minerals

Epidote with approximately 50 mol% of the Al_2Fe-end-member (also some REE-bearing epidote) and *titanite* (with small amounts of Al-F-titanite) are accessory minerals in the rocks. *Tourmaline* is a very frequent accessory mineral in the matrix, but it may also occur as a porphyroblast. Preliminary analyses indicate dravite-schorl solid solutions with negligible amounts of Ca.

Apatite

Another important accessory mineral is apatite. It can occur locally in large amounts and also in rather large crystals in aggregates with plagioclase ± epidote, in round or euhedral crystals (0.1 mm) with quartz and sulfate minerals, and in the matrix. Most crystals are rich in Cl (up to 6.52 wt%), some are enriched in F (up to 3.34 wt%). Those which are rich in Cl can also contain up to 1 wt% SrO, and some analyses also show up to 1 wt% SO_3. The Cl-poor apatite has a large range of F-contents (between 0.66 to 3.34 wt%, whereas the Cl-rich apatite is restricted to < 0.95 wt% F. These two types are also present in zoned crystals; cores and rims, however, may belong to either group.

Discussion

The protolith

It was shown above that the whole rock chemical composition is compatible with evaporite rocks. This interpretation is supported by the presence of sulfate minerals such as baryte and anhydrite, by tabular pseudomorphs after these minerals ("desert roses" and "bird tail shape"), by the presence of KCl and NaCl, and by the high contents of Sr in apatite. Furthermore, the metamorphic mineral association of kyanite + talc has been ascribed by Schreyer (1977) as indicative for metaevaporites. The original, sedimentary to diagenetic mineralogical composition of such evaporites was described by Braitsch (1962). He mentioned the authigenic formation of talc, often as the only phyllosilicate in anhydrite rocks and in NaCl-bearing rocks rich in anhydrite. Chlorite is also common, but restricted to non-carbonatic evaporites. Since the analyses of the metaevaporites from the Cóbdar area plot in the field of carbonate-free rocks (Fig. 8), chlorite and talc were probably important constituents of the protolith. It is interesting to note that in sedimentary-diagenetic salt deposits the mineral association illite + talc exists and these minerals could be the precursors of the high pressure assemblage phengite + talc (Chopin 1981; Massonne and Schreyer 1989). The matrix of the Cóbdar metaevaporites was formed by a prograde reaction from illite + chlorite ± quartz into biotite.

The peculiar pseudormophs of talc or quartz described above can be explained as relicts of sedimentary features. A diagenetic replacement of various evaporite minerals by talc was also described by Evans (1970) from Nova Scotia, and quartz pseudomorphs after anhydrite have been found by Arnold and Guillou (1981). Zimmermann (1907, quoted in Sonnenfeld 1984) observed that films of minute quartz crystals coat anhydrite crystals, which occur inside halite-forming pseudomorphs after gypsum. It is therefore possible that the features shown in Fig. 5 (increasing quartz grain size towards the center) and Fig. 6 represent the original sedimentary features. Other more irregular forms of mineral aggregates, such as plagioclase + apatite or quartz + sulfate + carbonate minerals, may have been amorphous silica, together with carbonate and possibly organic material, as fillings of geodes and of dissolved evaporite minerals.

Metamorphic conditions

Two different mineral parageneses in metapelites from the metaevaporite sequence, relevant for the near-peak metamorphic conditions, can be defined, based on textural relationships, mineral chemistry, and phase compatibilities. The first paragenesis includes the matrix minerals and all those porphyroblasts that are included by scapolite: Plagioclase, kyanite, talc, biotite, phengite, barroisitic amphibole, garnet, carbonate, and accessory minerals (paragonite and quartz might have been present at this stage, but these minerals could have formed later). The early formed minerals have been affected by a deformation which produced in some cases a slight foliation in the rocks, and also extensional veins.

The second paragenesis includes formation of scapolite and chlorite + quartz around the kyanite pseudomorphs. Coarse grained biotite and paragonite flakes (Fig. 4) in the pseudomorphs also formed later, because both minerals are present in those pseudomorphs where no kyanite and talc relicts are left.

A third paragenesis, less important for the high grade evolution and not discussed further, was formed on the

late stage retrograde path during brittle deformation in extensional veins, and includes albite, quartz, carbonate, and chlorite.

The metamorphic evolution in the high pressure stage is discussed in a simplified *P-T* diagram for metapelites (Fig. 12). The reaction curves were taken from experimental data by Massonne and Schreyer (1989), Holland (1979, 1988), Holdaway (1971),Chatterjee (1972). The triangular diagram Al-Mg + Fe-K + Na is chosen to illustrate the development of the phases. If a stable sequence of reactions is considered, phengite + talc were first formed at pressures above approximately 12 kbar. Chlorite + quartz might have persisted at pressures above 15 kbar, depending on the temperature. The presence of talc + kyanite and talc + phengite with Si = 3.3 indicates pressures near 18 kbar at temperatures between approximately 500 and 650°C. The breakdown of talc + phengite could have been produced by an increase in temperature or a decrease in pressure, to form biotite + kyanite + quartz + vapour (Massonne and Schreyer 1989). Temperatures must have been above 600°C, but the rocks studied here do not allow the derivation of a better estimate. Metabasites, studied in other areas of the Nevado-Filábride complex, indicated temperatures near 700°C at pressures near 15 (Puga et al. 1989) to 20 kbar (Galindo et al. 1991).

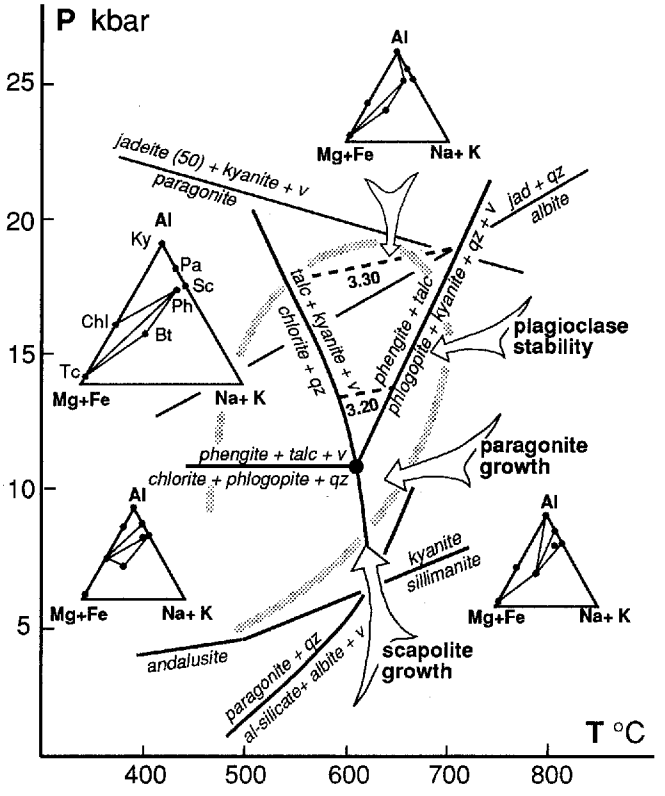

Fig. 12. *P-T* diagram for the high pressure evolution of the Cóbdar metaevaporites, constructed from experimental data (references are given in the text). Silicon contents in phengite of 3.3, *dashed line*, and the assemblage kyanite + phengite + talc indicate pressures near to the albite-jadeite-quartz equilibrium. Textural features in the samples suggest an early growth of plagioclase blasts, followed by paragonite and by scapolite growth, and by formation of chlorite + quartz in the kyanite pseudomorphs. The triangular diagrams Al - (Mg + Fe) - (Na + K) illustrate schematically the possible development of the phases (*Tc*, talc; *Chl*, chlorite; *Ky*, kyanite; *Pa*, paragonite; *Sc*, scapolite; *Ph*, phengite; *Bt*, biotite; *qz*, quartz; *v*, vapor). The inferred prograde evolution is hypothetical, and because of the limited mineralogical composition of the metaevorites, the peak and the retrograde metamorphic conditions can only be defined loosely

The albite-rich plagioclase porphyroblasts probably formed in a very early stage of decompression, when the rocks crossed the albite stability curve (Fig. 12). It is not clear whether there was another Na-mineral present in the rock at high pressures, which was subsequently replaced by albite. Barroisitic amphibole, which is more calcic toward the rim , is mostly present in rocks devoid of plagioclase. Relicts of omphacite were not found. The formation of paragonite in the pseudomorphs is also ascribed to the decompression path. Late stage chlorite + quartz formed when the rocks cooled below approximately 620 to 640°C at pressures between 6 and 12 kbar. Scapolite formation definitely occurred after the plagioclase growth, and probably during the onset of late stage chlorite + quartz formation.

Scapolite reactions

The well studied relationships between scapolite, calcite, and plagioclase (Evans et al. 1969; Orville 1975; Goldsmith and Newton 1977; Aitken 1983; Oterdoom and Wenk 1983) are not applicable to the Cóbdar locality, because the Cóbdar scapolites are rich in Na and poor in CO_3-component, and the textures clearly indicate that plagioclase is not consumed when scapolite is formed. Instead, biotite as the most important matrix mineral has almost completely disappeared in the areas of scapolite blastesis (Figs. 2 and 3). The necessary amounts of Na and Cl were possibly present in the rock either as solid NaCl or as a component of the mica. A possible reaction is a sliding reaction of the type:

$$2\,KMg_2Al_3Si_2O_{10}(OH)_2 + 1.25\,CaCO_3 + 2.75\,NaCl + 6.5\,SiO_2 = 1\,KMg_{2.5}Al_2Si_{2.5}O_{10}(OH)_2 + 1\,Ca_{1.25}Na_{2.75}Al_4Si_8O_{24}Cl_{0.75}(CO_3)_{0.25} + 1\,MgCO_3 + 0.5\,MgCl_2 + 1\,KCl + 1\,H_2O$$

This is a simplified reaction balanced with average compositions of scapolite and biotite neglecting the Cl-content in the original and in the late biotite, which also varies similarly to Al. The variation in Al^{VI} in biotite (Fig. 11) can be as large as 0.7 in a single sample. The magnesite, which appears in the schematic reaction, either forms dolomite with calcite, or talc or chlorite with SiO_2 and $SiO_2 + Al_2O_3$, respectively, which are readily available in the rocks. Calcium sulphate may replace $CaCO_3$ in the reaction to produce the small amounts of SO_4-scapolite, but probably most of the sulfate had already been dissolved during diagenesis.

Composition of the fluid phase

The reaction described above implies the presence of a fluid phase with high concentrations of salt during the

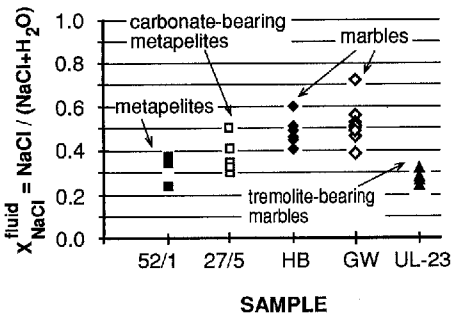

Fig. 13. Calculated composition of fluids from scapolite composition, based on experimental data by Ellis (1978)

decompression path of the rocks. The scapolite composition can be used as a monitor for the composition of the fluid phase (Ellis 1978), provided that other components such as SO_4 in scapolite, and $X(CO_2)$ and $X(F)$ in the fluid are low. It is based on an exchange equilibrium $NaCl_{s,cap} + CaCO_{3,cc} = CaCO_{3,scap} + NaCl_{fluid}$. The $X_{NaCl}(Fluid) = NaCl/(NaCl + H_2O)$ was calculated with the K_D-formulation given by Ellis (1978, his Fig. 9), valid for experimental conditions of 750°C/4 kbar, assuming ideal mixing in scapolite and in the fluid. Franz (1982) argued for a 'pseudoideal' behavior of NaCl-H_2O (from experimental data at 2 kbar, 590 to 670°C), and therefore this assumption is not too unrealistic. The average values for the different samples vary between $X_{NaCl} = 0.3$ and 0.5 (Fig. 13). This scatter reflects firstly the analytical uncertainty of the microprobe analyses. This is smaller than the observed range and we interpret the variation in X_{Nacl} as an indication for different concentrations of salt in the different rock types. Values in the order of 0.6 are near the saturation limit for the system H_2O-NaCl at the conditions of metamorphism. The X_{CO2} in the hydrous fluid is assumed to be low despite the presence of calcite + quartz. This assumption is made on the basis of experimental data on the immiscibility of CO_2- and NaCl-rich fluid phases (Yardley and Bottrell 1988; Johnson 1991). The occurrence of scapolite-free and scapolite-rich layers may therefore reflect the immiscibility of fluid phases (CO_2 and H_2O-NaCl), which prevented the original heterogeneous distribution of salt from being smoothed out by fluid circulation. The concentration of CO_2 in the fluid in the tremolite + calcite + scapolite lithologies may have been higher because they have a low X_{NaCl} (= 0.3) value calculated by the Ellis (1978) exchange equilibrium.

Other phases, which might give an indication of the fluid composition, are apatite and biotite. Both minerals contain Cl and F (Fig. 14; zoned apatites are not included). Biotite is rather variable in composition in both halogens, compatible with the interpretation that it changed its composition in a sliding reaction of the type mentioned above. The lack of any systematic variation between halogen contents in biotite-apatite pairs (which seem to be in textural equilibrium) probably indicates that they were formed with a fluid phase of variable composition in respect to F and Cl. The Cl content in apatite and in biotite depends strongly on the salt concentration in the coexisting solution (Zhu and Sverjensky 1991). However, more systematic analyses would be necessary to quantify the fluid-apatite-biotite relations. The presence of some Sr, SO_4, and possibly CO_3 in the apatites will also complicate these relations.

Munoz (1984, 1992) developed a method to derive fugacity ratios of HF and HCl in a fluid, coexisting with biotite, based on F-Cl-OH exchange equilibria of F-, Cl-, and OH-biotite endmembers. This method takes into ac-

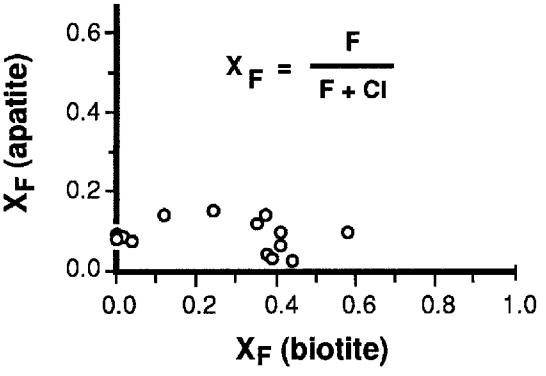

Fig. 14. Comparison of F- and Cl-contents in coexisting (textural equilibrium) apatite and biotite. The lack of a systematic correlation probably indicates chemical disequilibrium

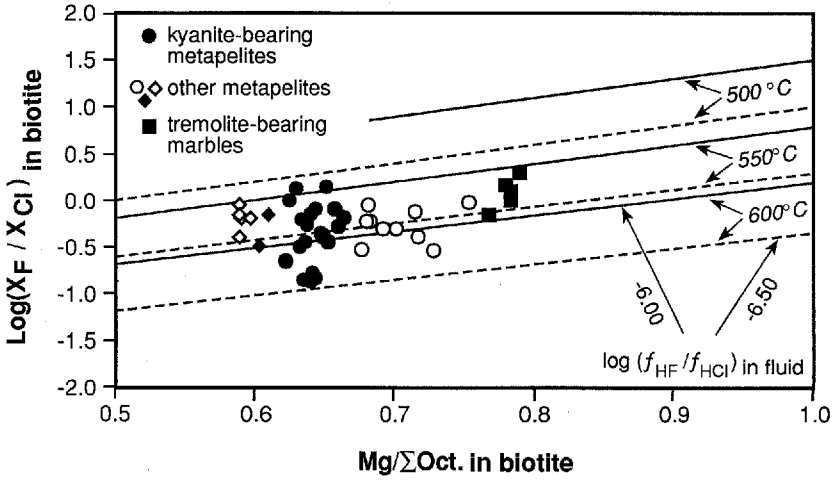

Fig. 15. F-Cl ratios in biotite as a function of biotite composition on octahedral sites. *Diagonal lines* are reference isopleths for two sets of log (f_{HF}/f_{HCl}) values in the fluid (Munoz 1992) at assumed equilibrium temperatures between 500 and 600°C (see text for discussion)

count the Mg/(Mg + Fe) ratio and the Al^{VI} content of biotite and uses the F and Cl contents, measured by electron microprobe. The values for the biotites from the Cóbdar metaevaporites are shown in Fig. 15, together with reference lines for constant fugacity ratios in the fluid at assumed metamorphic temperatures of 500, 550, and 600°C. The data show that the temperature estimate for the major equilibration stage of 550 to 600°C (Fig. 12) is realistic. Secondly, they confirm the dependency of F-Cl-distribution in biotite on X_{Mg}. The variation within a single sample is probably due to a combined effect of temperature and pressure variation and differing F- and Cl-activities.

Conclusions

There is little doubt that the metamorphosed rocks were originally evaporites, indicating a near continental or shallow marine environment. It is not compatible with the hypothesis that the metabasites of the Cóbdar area are part of a dismembered ophiolite complex (cf., Bodinier et al. 1987).

It is unlikely that the basic intrusions initiated hydrothermal convection cells responsible for scapolitization (as described by Vanko and Bishop 1982), because the bodies are relatively small. Also, the intrusions are clearly pre-metamorphic, whereas scapolite grew during the metamorphic decompression. Scapolite was not produced by metasomatic reactions of a fluid phase, which might have come from any other (unknown) source. This is indicated by the irregular distribution of scapolite in the rocks and the absence of indications for large scale (> 10 cm) metasomatism, such as monomineralic zones. Though the metaevaporites show some deformation, this is mostly restricted to brittle-ductile transitional features at lithological boundaries. Shear zones, which can act as metamorphic aquifers (e.g., Selverstone et al. 1991) are not present. Wherever ductile deformation is observed, these rocks show essentially the same mineralogical composition as the undeformed ones and no relation to the scapolite formation. The small grain size of the rock could be taken as an argument to explain the whole sequence as an ultramylonite. This is, however, not consistent with the outcrop situation (Fig. 1) and especially not with the preservation of pseudomorphs.

We argue therefore for a similar origin of scapolite as proposed by Hietanen (1967) and Mora and Valley (1989), who suggested that scapolite crystallized during regional metamorphism in rocks which had originally contained halite. The exact mechanism of scapolite formation, however, seems to be different, because the reaction includes breakdown of biotite instead of plagioclase, and the production of H_2O. Plagioclase formed earlier in the rocks than scapolite, possibly by different reactions. Though the rocks have been metamorphosed at high pressures, scapolite was formed rather late during uplift.

The stability field of NaCl-rich scapolites is not well known, because experimental studies are not available. The marialite NaCl-endmember can be synthesized at low to high pressures and high temperatures (> approximately 700 to 800°C (Eugster and Prostka 1960; Newton and Goldsmith 1975)). Orville (1975) and Ellis (1978) found that a high activity of NaCl is necessary to stabilize scapolite over plagioclase + calcite + NaCl at 4 kbar, 750°C, but the scapolites always contained a certain amount of X_{An} component. Ellis (1978) used NaCl/(NaCl + H_2O) concentrations of up to 0.8. At higher NaCl concentrations, scapolite can be formed, but the phase relations become complicated by other phases (cancrinite, melt: Orville 1975). Vanko and Bishop (1982) synthesized scapolite with eqAn = 18 mol% at 1.7 to 2.8 kbar and 600 to 750°C. These experimental results are in general agreement with our conclusion, that high NaCl concentrations favored scapolite formation. Oterdoom and Wenk (1983) derived an empirical phase diagram. It shows a plagioclase + calcite + $NaCl_{aq}$ phase field at conditions where the Cóbdar scapolites have formed. We assume that the NaCl concentrations in the rocks described by Oterdoom and Wenk (1983) were not high enough for scapolite formation.

The early albite and the late scapolite growth in the Cóbdar metaevaporites is thus explained in the following way:

At high pressures and temperatures near 18 kbar, 600°C or higher, NaCl must have been present as solid halite. It is not clear if the rock was dry or fluid poor. Decreasing pressures produced small amounts of H_2O by breakdown of the phengite component of matrix white mica. The fluid must have been heterogeneous, because salt was probably heterogeneously distributed in the rock, as was the distribution of the H_2O producing phengite. This heterogeneity is reflected by the variable mineral composition (Figs. 13–15), though varying P and T also have contributed to the variation. The white mica reacted with the fluid firstly to form plagioclase (essentially albite). A simplified reaction is:

$$KAlMgSi_4O_{10}(OH)_2 + 0.33\,SiO_2 + NaCl = NaAlSi_3O_8 + 0.33\,Mg_3Si_4O_{10}(OH)_2 + 0.66\,H_2O + KCl\,.$$

(Also, breakdown of Na-pyroxene or Na-amphibole might have produced albite and kyanite reaction to paragonite in a similar manner.) The biotite-scapolite reaction took place at significantly lower pressure. Albite was not consumed during scapolite formation because it is stable together with scapolite + calcite + halite (Fig. 9 in Orville 1975). The albite forming reaction first produced a saturated or nearly saturated brine. As the scapolite reaction proceeds, the brines become more and more undersaturated until the reaction finally stopped.

Acknowledgements. This study was supported by grants from MEC (Spain) and DAAD (Germany) (Acciones Integradas awards) and NATO. We thank F. Galbert (ZELMI, TUB), M.A. Hidalgo (Servicios Técnicos Univ. Granada), and P. Hill and S. Kearns (Microprobe Unit of the Department of Geology of Edinburgh), and F. Cámara (Department of Mineralogy and Petrology, Granada) for their help with the microprobe analyses. The SEM pictures and XRF analyses were made in the Servicios Técnicos of the Univ. Granada. We thank J.M. Fernandez-Soler (Department of Mineralogy and Petrology, Granada) and I. Guerra for their help with the XRF analyses and the SEM studies respectively. Discussions with

W. Heinrich and his critical reading of an early version of the manuscript helped to clarify many points. We thank R. Oberhänsli and E. Grew for their constructive reviews.

References

Aitken BG (1983) T-X_{CO2} stability relations and phase equilibria of a calcic carbonate scapolite. Geochim Cosmochim Acta 47:351–362

Arnold M, Guillou JJ (1981) Les filons métallifères hercyniens. Origine de l'anhydrite et mécanisme de la pseudomorphose subséquente: proposition d'un modèle. Sci Terre 24:173–195

Balanya JC, García-Dueñas V (1986) Grandes fallas de contracción y de extensión implicadas en el contacto entre los dominios de Alborán y Sudibérico en el Arco de Gibraltar. Geogaceta 1:19–20

Bodinier JL, Morten L, Puga E , Diaz de Federico A (1987) Geochemistry of metabasites from the Nevado-Filábride Complex, Betic Cordilleras Spain: relics of a dismembered ophiolitic sequence. Lithos 20:235–245

Braitsch (1962) Entstehung und Stoffbestand der Salzlagerstaetten. Springer-Verlag, Berlin Heidelberg New York

Chamberlain CP, Docka A, Post JE, Burnham ChW (1985) Scapolite: alkali atom configuration, antiphase domains, and compositional variations. Am Mineral 70:134–140

Chatterjee ND (1972) The upper stability limit of the assemblage paragonite + quartz and its natural occurrences. Contrib Mineral Petrol 42:259–271

Chopin Ch (1981) Talc-phengite: a widespread assemblage in high grade pelitic blueschist of western Alps. J Petrol 22:628–650

Egeler CG (1963) On the tectonics of the Eastern Betic Cordilleras. Geol Rundsch 53:260–269

Ellis DE (1978) Stability and phase equilibria of chloride and carbonate-bearing scapolites at 750°C and 4000 bar. Geochim Cosmochim Acta 42:1271–1281

Eugster H, Prostka HJ (1960) Synthetic scapolites (abstract). Bull Geol Soc Am 71:1858

Evans G (1970) Genesis of sylvite- and carnallite-bearing rocks from Wallace Nova Scotia In: Ron JL, Dellwing LF (eds) 3rd Symp Salt 1:239–245

Evans BW, Shaw DM, Haugton DR (1969) Scapolite stoichiometry. Contrib Mineral Petrol 24:295–305

Franz G (1982) The brucite-periclase equilibrium at reduced H_2O activities: some information about the system H_2O-NaCl. Am J Sci 282:1325–1339

Galindo-Zaldivar J (1990) Geometría y cinemática de las deformaciones neógenas en Sierra Nevada (Cordilleras Béticas). Thesis Univ Granada

Galindo J, Gonzalez-Lodeiro F, Gómez-Pugnaire MT, Jabaloy A, Julivert M (1991) Introduction to the geology of the Betic Cordilleras. ICE Univ Granada

Goldsmith JR, Newton RC (1977) Scapolite-plagioclase stability relations at high-pressures and temperatures in the system $NaAlSi_3O_8$-$CaAl_2Si_2O_8$-$CaCO_3$-$CaSO_4$. Am Mineral 62:1063–1081

Gómez-Pugnaire MT (1981) Evolución del metamorfismo alpino en el Complejo Nevado-Filábride de la Sierra de Baza (Cordilleras Béticas España). Tecniterrae 4:1–130

Gómez-Pugnaire MT, Cámara F (1990) La asociaciòn de alta presión distena + talco + fengita coexistente con escapolita en metapelitas de origen evaporítico Complejo Nevado-Filábride (Cordilleras Béticas). Rev Soc Geol Esp 8:87–96

Gómez-Pugnaire MT, Fernandez-Soler JM (1987) High-pressure metamorphism in metabasites from the Betic Cordilleras (SE Spain) and its evolution during the alpine orogeny. Contrib Mineral Petrol 95:231–244

Gómez-Pugnaire MT, Sassi F , Visonà D (1978) Sobre la presencia de paragonita y pirofilita en las filitas del Complejo Nevado-Filábride en la Sierra de Baza (Cordilleras Béticas España). Bol Geol Mineral 89:468–474

Gómez-Pugnaire MT, Fontboté JM, Sassi FP (1981a) On the occurence of a metaconglomerate in the Sierra de Baza (Nevado-Filábride Complex, Betic Cordilleras, Spain). Neues Jahrb Geol Paläont Monatsh 3:176–180

Gómez-Pugnaire MT, Torres-Ruiz J, Martinez-Martinez JM (1981b) Escapolita en rocas de las series permotriásicas del Complejo Nevado-Filábride (Cordilleras Béticas). Algunas consideraciones sobre su origen. Bol Soc Esp Mineral 4:37–46

Hietanen AH (1967) Scapolite in the Belt Series in the St. Joe-Clearwater region Idaho. Geol Soc Am Spec Pap 86

Hogarth DD, Griffin WL (1978) Lapis lazuli from Baffin Island – a Precambrian meta-evaporite. Lithos 11:37–60

Holdaway MJ (1971) Stability of andalusite and the aluminium silicates phase diagram. Am J Sci 271:91–131

Holland TJB (1979) Experimental determination of the reaction paragonite = jadeite + kyanite + H_2O and internally consistent thermodynamic data for part of the system Na_2O - Al_2O_3 - SiO_2 - H_2O with application to eclogites and blueschists. Contrib Mineral Petrol 68:293–301

Holland TJB (1988) Preliminary phase relations involving glaucophane and applications to high pressure petrology: new heat capacity and thermodynamic data. Contrib Mineral Petrol 99:134–142

Jabaloy A (1991) La estructura de la región occidental de la Sierra de los Filabres. Thesis Univ Granada

Johnson EL (1991) Experimentally determined limits for H_2O-CO_2-NaCl inmiscibility in granulites. Geology 19:925–928

Jong De K (1991) Tectono-metamorphic studies and radiometric dating in the Betic Cordilleras (SE Spain). Proefsch Vrije Univ Amsterdam

Jong De K, Bakker H (1991) The Mulhacen and Alpujarride Complex in the eastern Sierra de los Filabres SE Spain: litho-stratigraphy. Geol Mijnbouw 70:93–103

Massonne H J, Schreyer W (1989) Stability field of the high-pressure assemblage talc + phengite and two new phengite geobarometers. Eur J Mineral 1:391–410

Moecher DP, Essene EJ (1991) Calculation of CO_2 activities using scapolite equilibria: constraints on the presence and composition of a fluid phase during high grade metamorphism . Contrib Mineral Petrol 108:219–240

Moine B, Sauvan P, Jarousse J (1981) Geochemistry of evaporite-bearing series: a tentative guide for the identification of metaevaporites. Contrib Mineral Petrol 76:401–412

Mora CI, Valley JW (1989) Halogen-rich scapolite and biotite: implications for metamorphic fluid-rock interaction. Am Mineral 74:721–737

Munoz JL (1984) F-OH and Cl-OH exchange in micas with application to hydrothermal ore deposits. In: Bailey SW (ed) (Reviews in mineralogy 13: Micas) Mineral Soc Am, Washington, DC, pp 469–493

Muñoz M (1986) Estudio comparativo de los cuerpos intrusivos básicos asociados a los materiales de edad triásica de los dominios Subbético y Nevado-Filábride del sector centro-oriental de las Cordilleras Béticas. Geogaceta 1:35–37

Munoz JL (1992) Calculation of HF and HCl fugacities from biotite compositions: revised equations (abstract). Geol Soc Am Abstr Program 24:A221

Newton RC, Goldsmith JR (1975) Stability of the scapolite meionite (3 $CaAl_2Si_2O_2$-$CaCO_3$) at high pressures and storage of CO_2 in the deep crust. Contrib Mineral Petrol 49:49–62

Nijhuis HJ (1964) Plurifacial alpine metamorphism in the south-eastern Sierra de los Filabres South of Lubrín. Thesis Univ Amsterdam

Orville Ph (1975) Stability of scapolite in the system Ab-An-NaCl-$CaCO_3$. Geochim Cosmochim Acta 39:1091–1105

Oterdoom WH, Wenk HR (1983) Ordering and composition of scapolite: field observations and structural interpretation. Contrib Mineral Petrol 23:230–241

Puga E, Diaz de Federico A, Fediukova E, Bondi M, Morten L (1989) Petrology, geochemistry, and metamorphic evolution of the ophiolitic eclogites and related rocks from the Sierra Nevada

(Betic Cordilleras, Southeastern Spain). Schweiz Mineral Petrogr Mitt 69:435–455
Schreyer W (1977) Whiteschists: their compositions and pressure-temperature regimes based on experimental field and petrographic evidence. Tectonophysics 43:127–144
Selverstone J, Morteani G, Staude J-M (1991) Fluid channeling during ductile shearing in transformation of granodiorite into aluminous schists in the Tauern Window, Eastern Alps. J Metamorphic Geol 9:419–431
Serdyuchenko DP (1975) Some Precambrian scapolite-bearing rocks evolved from evaporites. Lithos 8:1–7
Sonnenfeld P (1984) Brines and evaporites. Acad Press, London
Trommsdorf V, Skippen G, Ulmer P (1985) Halite and sylvite as solid inclusions in high-grade metamorphic rocks. Contrib Mineral Petrol 89:24–29
Vanko DA, Bishop FC (1982) Occurrence and origin of marialitic scapolite in Humboldt Lopolith, N.W. Nevada. Contrib Mineral Petrol 81:277–289
Vissers R L (1982) A structural study of the central Sierra de los Filabres (Betic Zone, SE Spain) with emphasis on deformational processes and their relation to the Alpine metamorphism. GUA Pap Geol 2:5–154
Voet HW (1967) Geological investigations in the northern Sierra de los Filabres around Macael and Cóbdar, south-eastern Spain. Thesis Univ Amsterdam
Yardley BWD, Bottrell SH (1988) Inmiscibility fluids in metamorphism: implications of two phase flow for reaction history. Geology 16:199–202
Zhu CH, Sverjensky DA (1991) Partitioning of F-Cl-OH between minerals and hydrothermal fluids. Geochim Cosmochim Acta 55:1837–1858

Editorial responsibility: W. Schreyer